



RESEARCH LETTER

10.1002/2014GL061251

Key Points:

- Supercontinent clusters of subducting slabs are unstable to rollback
- The slab rollback instability disperses continents
- The dispersal time is commensurate with the Wilson cycle period

Correspondence to:

D. Bercovici,
david.bercovici@yale.edu

Citation:

Bercovici, D., and M. D. Long (2014), Slab rollback instability and supercontinent dispersal, *Geophys. Res. Lett.*, *41*, doi:10.1002/2014GL061251.

Received 17 JUL 2014

Accepted 26 AUG 2014

Accepted article online 28 AUG 2014

Slab rollback instability and supercontinent dispersal

David Bercovici¹ and Maureen D. Long¹¹Department of Geology and Geophysics, Yale University, New Haven, Connecticut, USA

Abstract Supercontinents coalesce over subduction zone complexes and their subsequent dispersal is usually attributed to heating and upwelling of continent-insulated mantle. This dispersal mechanism, however, requires considerable mantle internal heating. Alternatively, the supercontinent configuration may be mechanically unstable and disperse regardless of heating mode. In particular, increased drag on plates or subducting slabs (e.g., by accumulating continents) causes them to slow down and trenches to rollback. Once subcontinental slabs are slightly separated, resistance to their descent increases, inducing further trench migration. Slabs thus undergo a rollback instability, which disperses supercontinents. A simple theoretical model illustrates this instability and shows that there are two equilibrium states, one unstable supercontinent state where slabs are conjoined and one stable state where slabs are widely separated. Slab rollback from the unstable to stable states occurs at typical slow tectonic speeds and over a period commensurate with the age of ocean basins and the Wilson cycle.

1. Introduction

The Wilson Cycle is one of the basic tenets of plate tectonic evolution and describes the process of supercontinent agglomeration and dispersal [Wilson, 1966]. The driving mechanism for this cycle is traditionally attributed to the accumulation of continental crust over mantle downwellings (or complexes of subducting slabs) and the subsequent heating of the subcontinental mantle because of supercontinent insulation, which eventually drives an upwelling that disperses the supercontinent [Anderson, 1982; Gurnis, 1988; see also Yoshida, 2010, 2012, 2013; Yoshida and Santosh, 2011; Lenardic et al., 2011; Rolf and Tackley, 2011; Rolf et al., 2012, 2014]. This scenario, however, relies on active internal heating of the mantle by radiogenic sources [e.g., Gurnis, 1988; Lenardic et al., 2011; c.f., Yoshida, 2013; Rolf et al., 2014]. If the mantle energy source is primarily from primordial heat, i.e., its Urey number is very low [Korenaga, 2008; Jaupart et al., 2007], then the heating of the subcontinental mantle could be too weak to induce dispersal [e.g., Heron and Lowman, 2011].

We propose an alternative hypothesis for supercontinental dispersal that is independent of mantle heating mode. In particular, a major convergence zone drawn together by a large complex of downwellings is potentially unstable for purely mechanical reasons. First, divergent stress associated with thick continental crust opposes lithospheric convergence and slows plate motion, which causes the downwelling slabs to recede from each other, since the plates cool and become heavier closer to their spreading centers. As subcontinental slabs become more separated, the mantle between them induces greater viscous resistance, slows the slabs, and plates further, hence causing further rollback. The plates and slabs, therefore, undergo a rollback instability, which disperses the supercontinent. In this paper we illustrate the physics of this supercontinent rollback instability with a simple theoretical model and show that the predicted speed and time scale for dispersal are commensurate with the Wilson cycle.

2. Theory

Conditions for slab rollback have been studied extensively by Stegman et al. [2006, 2010] [see also Schellart et al., 2007, 2008; Clark et al., 2008], and while rollback form and evolution depends on plate strength, trench width, coupling to the overriding plate, and induced 3-D (especially toroidal) flow [Kincaid and Griffiths, 2003; Funicello et al., 2006; Pironallo et al., 2006; Stegman et al., 2010; Gerya and Meilick, 2011], a fundamental cause for rollback is excess negative buoyancy of the subducting plate [Stegman et al., 2010]. Here we develop a simple analytical boundary layer model to illustrate the supercontinent rollback instability. In particular, we show how slab and plate velocity are affected by the supercontinent configuration, which in turn alters the plate's negative buoyancy, convective stability, and, ultimately, its length.

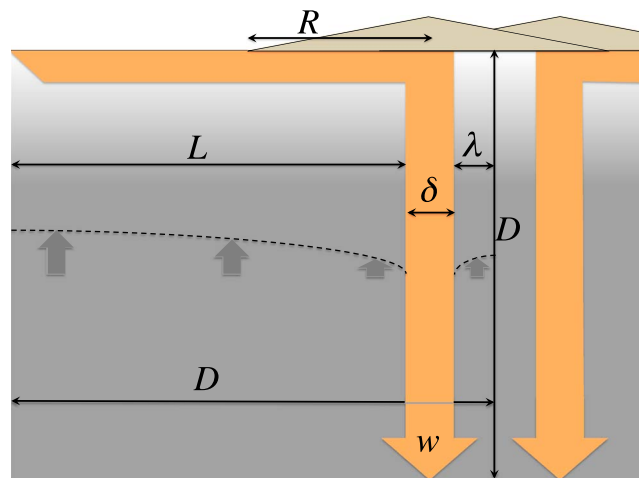


Figure 1. Sketch of model configuration and geometry. See text for discussion.

We consider a simple configuration of two mirror-image sinking slabs (Figure 1), with symmetry points below the ridge at $x = 0$ and at the mutual convergence point $x = D$, where we assume the total cell width equals the mantle thickness D . The length of the plate to the slab is L , the slab width is δ , and once the slabs separate, the gap between them has half-width λ . Although L and λ are time dependent, we require $L + \delta + \lambda = D$.

2.1. Plate Length and Trench Position

In our idealized model, subduction occurs where the top thermal boundary layer or plate goes convectively unstable. (The lithosphere is not considered inordinately strong since we assume some preweakening or self-weakening and/or

damage mechanism [Bercovici and Ricard, 2012, 2014] has made it pliable enough to subduct [e.g., Gurnis et al., 2004; Nikolaeva et al., 2010]). The subducting slab thickness δ is given by equating the local Rayleigh number of the boundary layer to the critical Rayleigh number for the onset of convection [Howard, 1966; Solomatov, 1995]:

$$\frac{\rho g \alpha \Delta T \delta^3}{\mu_0 \kappa} = \mathcal{R}_c \quad (1)$$

where ρ is mantle density, g gravity, α thermal expansivity, ΔT the lithospheric temperature drop, μ_0 the upper mantle viscosity (which first resists the instability), κ thermal diffusivity, and $\mathcal{R}_c \approx 660$ is the critical Rayleigh number for a free-slip surface [Chandrasekhar, 1961]. Although δ is a system constant, it is related to plate age by $\delta = 2\sqrt{\kappa L/w}$ [e.g., Solomatov, 1995] and thus the plate length is

$$L = \frac{\delta^2}{4\kappa} w \quad (2)$$

where w is the slab's descent velocity, which is assumed the same as the plate velocity. Although subduction on Earth is more complex than implied here, and indeed there is a wide distribution of subduction ages [e.g., Becker et al., 2009], the relation (2) captures the basic process whereby if the slab and plate slow down, the plate becomes heavier and the trench retreats.

2.2. Ambient Mantle Flow and Resistance

If the model slabs become separated by a gap, the flow of the mantle inside the gap and behind the slabs provide viscous resistance to slab descent. Widening of the gap increases viscous resistance; hence, the plates slow down and cause the gap to widen further.

We consider the resistance to vertical descent of just one of the model slabs, since the other slab is its mirror image. We treat the vertical flow as Poiseuille flow wherein the slab's velocity $-w$ imposes a no-slip boundary condition on either of the slab's vertical surfaces (on the plate and gap sides at $x = L$ and $x = L + \delta$), while the symmetry points (below the ridge at $x = 0$ or mutual convergence point $x = D$) involve reflecting boundary conditions. On either side of the slab the vertical velocity is given generically by

$$v_z = -w - \frac{1}{2\mu} \frac{dp}{dz} (b-x)(b+x-2a) \quad (3)$$

where μ is the mean viscosity of the whole mantle, which is dominated by the lower mantle's value, dp/dz is a nonhydrostatic pressure gradient driving mantle return flow induced by the downward slab flux, and a and b are the positions of the reflecting and no-slip surfaces, respectively (i.e., $dv_z/dx = 0$ at $x = a$ and $v_z = -w$ at $x = b$). For the mantle below the plate, $a = 0$ and $b = L$, and for the mantle in the gap between slabs, $a = D$ and $b = D - \lambda = L + \delta$. We assume that the pressure gradient is the same on both sides of the slab, i.e., due to build up of slab material at depth; moreover, this pressure gradient is determined by mass

conservation wherein there is no net vertical mass flux across any horizontal surface in the cell. Integrating the vertical velocity from $x = 0$ to D , including that of the slab and both regions of mantle on either side of it, yields

$$-\frac{1}{2\mu} \frac{dp}{dz} = \frac{3}{2} \frac{D}{\lambda^3 + L^3} w \quad (4)$$

2.3. Continental Accumulation and Resistance

We consider the accumulation of a finite 2-D volume of buoyant unsubductable continental “fluid” of thickness h , density ρ_c , and viscosity μ_c , wherein the continental mass collapses if the underlying convergence ceases. The equation for a viscous 2-D gravity current of thickness h with a free-slip surface and a no-slip base moving at a horizontal velocity $v(x)$ is

$$\frac{\partial h}{\partial t} + v \frac{\partial h}{\partial x} = \frac{\rho' g}{3\mu_c} \frac{\partial}{\partial x} \left(h^3 \frac{\partial h}{\partial x} \right) - h \frac{dv}{dx} \quad (5)$$

[Huppert, 1982] where $\rho' = (\rho - \rho_c)\rho_c/\rho$ is the isostatically reduced crustal density [Didden and Maxworthy, 1982]. We assume the continental gravity current has an approximately self-similar shape near the downwelling slab and is given by $h(x, t) = H(t)f(\zeta)$, where $\zeta = (x - L - \delta/2)/R$ (i.e., to the left of the slab $\zeta < 0$), H is the characteristic height, f is a dimensionless shape function, and R is the half-length of the current’s base (Figure 1). The current’s volume is conserved; thus, the half-volume (per unit length into the plane) $V = H(t)R(t) \int_{-1}^0 f(\zeta) d\zeta$ is a constant; we can define $\int_{-1}^0 f d\zeta = 1$ such that $H(t) = V/R(t)$. As we will later consider perturbations to a steady state, we assume the shape $f(\zeta)$ approximates that of the steady critical wedge in which the advection term on the left balances the gravity collapse (i.e., nonlinear diffusion) term on the right of (5); in this case, and satisfying the volume integral constraint on f , we find $f(\zeta) \approx \frac{4}{3}(1 + \zeta)^{1/3}$ for $\zeta < 0$. Substituting $h = \frac{V}{R}f(\zeta)$ into (5), evaluating it near the center of the gravity current ($\zeta \approx 0$) where we assume $dh/dx = 0$ and $dv/dx \approx -w/\delta$, we obtain

$$\frac{dR}{dt} = \frac{c\rho'gV^3}{\mu_c} \frac{1}{R^4} - \frac{w}{\delta} R \quad (6)$$

where $c = 2^7/3^6 \approx 0.18$. The stress of the continental gravity current acting against the top of the plate is $\tau_c = -\rho'gh \frac{dh}{dx}$ and the force (per unit length into the plane) acting against the plate is

$$F_c = \int_{L+\delta/2-R}^{L+\delta/2} \tau_c dx = -\frac{8\rho'gV^2}{9R^2} \quad (7)$$

2.4. Mechanical Work Balance

The evolution of plate length is inferred from the balance of mechanical work on the slab; i.e., the release of gravitational potential energy of the slab is balanced by viscous work done by the mantle on either side of the slab and by the drag of the continental pile against the plate. In equilibrium, the steady subduction rate w allows for this energy balance. But if the trench recedes at a rate $-dL/dt$, then the slab swings down and drops a distance $|dL|$ in time dt and releases additional gravitational energy. The total energy balance is

$$\begin{aligned} \rho g \alpha \frac{1}{2} \Delta T \delta \left(w - \frac{dL}{dt} \right) &= \mu w \left[\frac{dv_z}{dx} \right]_L^{L+\delta} + 2\gamma \mu \left(\frac{1}{L} + \frac{1}{\lambda} \right) \left(\frac{dL}{dt} \right)^2 - \frac{1}{D} \int_{L+\delta/2-R}^{L+\delta/2} \tau_c v_x dx \\ &= 3\mu \frac{D(D-\delta)}{\lambda^3 + L^3} w^2 + 2\gamma \mu \frac{D-\delta}{L\lambda} \left(\frac{dL}{dt} \right)^2 + \frac{8\rho'gV^2}{9D} \frac{w}{R^2} \end{aligned} \quad (8)$$

where $\Delta T/2$ is the slab’s mean thermal anomaly, and we assume the plate velocity v_x is constant up to the trench and equal to the slab velocity w . The fraction γ accounts for how much of the mantle is involved with rollback dissipation; e.g., if portions of the slab are anchored in the lower mantle (e.g., due to higher lower mantle viscosity), then they participate less in rollback, in which case γ is small.

Table 1. Material and Model Properties

Quantity	Symbol	Value
Density, mantle	ρ	3300 kg/m ³
Density, continent	ρ_c	2700 kg/m ³
Gravitational acceleration	g	10 m/s ²
Thermal expansivity	α	$3 \times 10^{-5} \text{ K}^{-1}$
Thermal diffusivity	κ	$10^{-6} \text{ m}^2/\text{s}$
Lithosphere temperature drop	ΔT	1400 K
Viscosity, upper mantle	μ_0	10^{21} Pa s
viscosity, mean mantle	μ	$30\mu_0$
Viscosity, continent	μ_c	μ_0
Mantle depth	D	3000 km
Continent 2-D volume	V	$40 \text{ km} \cdot D/3$

2.5. Dimensionless Governing Equations

We nondimensionalize length by δ and time by $\delta^2/(4\kappa)$, such that $w = (4\kappa/\delta)u$, $L = \delta^2 w/(4\kappa) = \delta u$, and $R = \delta r$, in which case the governing equations (8) and (6) become

$$\frac{du}{dt} = u \left(1 - \frac{C}{r^2} - \frac{3B\eta u}{u^3 + (\eta - u)^3} \right) - \frac{2\gamma B}{u(\eta - u)} \left(\frac{du}{dt} \right)^2 \quad (9a)$$

$$\frac{dr}{dt} = \frac{\mathcal{K}^5}{r^4} - ur \quad (9b)$$

where

$$\eta = \frac{D}{\delta}, \quad B = \frac{8\eta\mu}{\mathcal{R}_c\mu_0},$$

$$C = \frac{16\rho'V^2}{9\rho\alpha\Delta T\delta^3D},$$

$$\text{and } \mathcal{K}^5 = \frac{c\rho'gV^3}{4\kappa\mu_c\delta^3} \quad (10)$$

and we have assumed for simplicity that $\eta \gg 1$ in developing (9). The dimensionless parameters represent the aspect ratio between convection cell size and slab thickness η , the mantle drag on the slab B , the continental drag on the plate C , and the collapse rate of the continent \mathcal{K} . Using $\mathcal{R}_c \approx 660$ and typical model properties (see Table 1), then $\eta \approx 40$, while B , C , and \mathcal{K} are all $O(10)$.

3. Analysis

3.1. Equilibrium States

Apart from the null solution, the steady state solution u_0 to (9) satisfies

$$(1 - \nu u_0^{2/5})(3u_0^2 - 3\eta u_0 + \eta^2) - 3B u_0 = 0 \quad (11)$$

where $\nu = C/\mathcal{K}^2$, which, given the typical sizes of C and \mathcal{K} , is a small number. If we assume $\nu \ll 1$, then the two steady solutions are simply

$$u_0 = \frac{1}{2}(\eta + B) \pm \frac{1}{2}\sqrt{(\eta + B)^2 - \frac{4}{3}\eta^2} \quad (12)$$

Viable solutions are limited by the conditions that $u_0 \leq \eta$ and that u_0 is real; these imply that $2/\sqrt{3} - 1 \leq B/\eta \leq 1/3$, which, by (10), corresponds to a plausible viscosity ratio range of $13 \leq \mu/\mu_0 \leq 28$. For the upper limit $B/\eta = 1/3$, solutions are

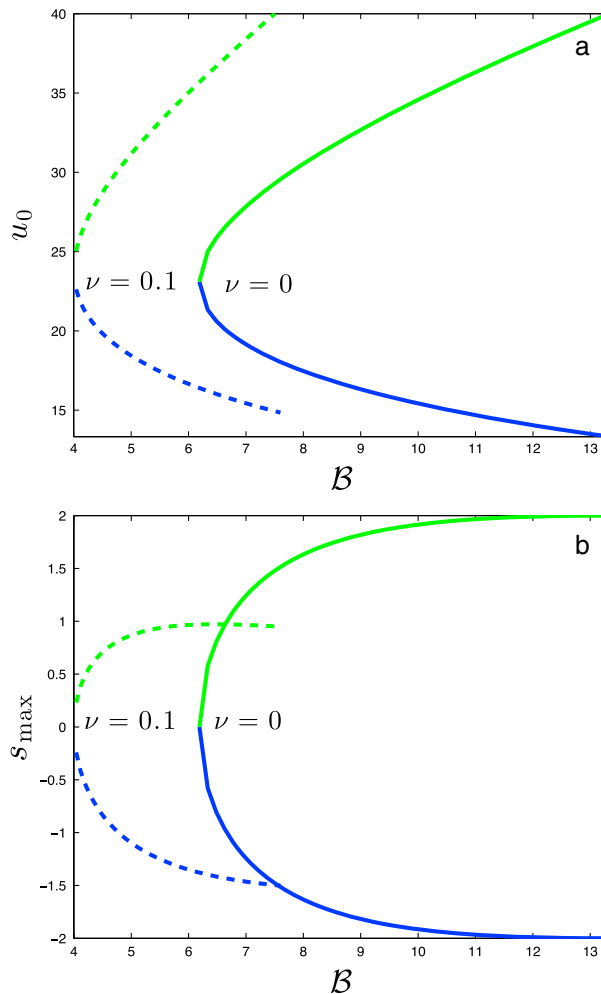


Figure 2. (a) Solutions u_0 to the steady state condition (11) and (b) the maximum growth rate s_{\max} of perturbations to these solutions versus the parameter B for select values of $\nu = C/\mathcal{K}^2$, with $\mathcal{K} = 10$ and $\eta = 40$. The upper (green) branch is the long-plate solution, which is unstable ($s_{\max} > 0$), and the lower (blue) branch is the shorter plate solution, which is stable ($s_{\max} < 0$).

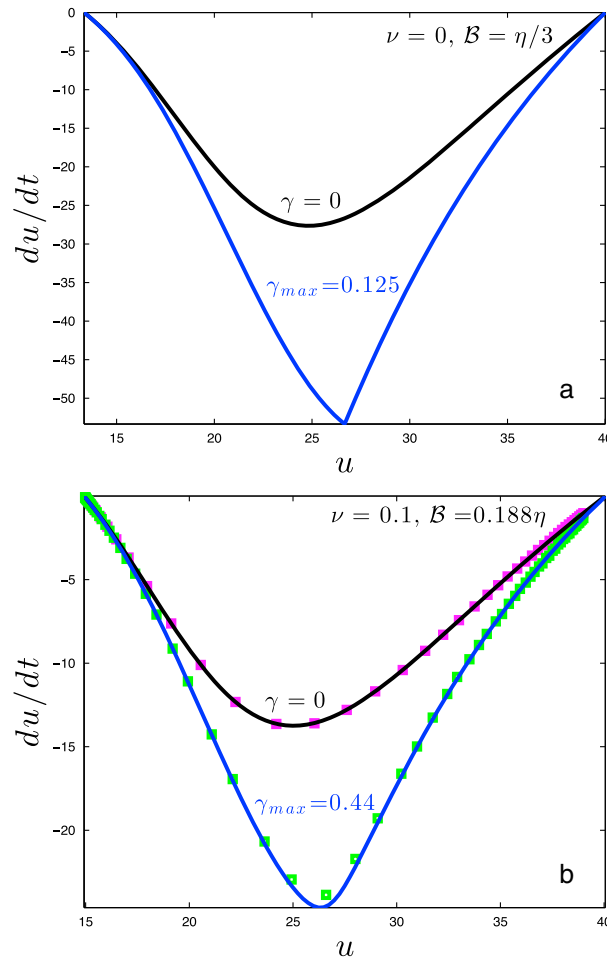


Figure 3. Samples of rollback velocity du/dt as a function of plate length u from solutions to (9). Cases are shown for values of B that yield the equilibrium solutions $u_0 \approx (2 \pm 1)\eta/3$, (a) one for $\nu = C/\mathcal{K}^2 = 0$ and no continental drag and (b) one for $\nu = 0.1$ and finite continental drag. The curves shown are for γ when the viscous dissipation of rollback is negligible (i.e., $\gamma = 0$, black curve) and for the maximum allowable value of γ (i.e., maximum rollback dissipation) that still allows real solutions for du/dt from (15) (blue curve). For the cases with $\nu = 0$ the relations are exact. For the cases with $\nu > 0$, the solid curves are solutions to (9) assuming $dr/dt = 0$ such that $r = \mathcal{K}u^{-1/5}$; the square colored symbols are from the full numerical integration of (9), which verifies that $dr/dt \approx 0$ is a reasonable assumption.

$u_0 = (2 \pm 1)\eta/3$; i.e., either the plate is at the full possible length or has rolled back to 1/3 its full length. (For the lower limit, there is only one solution $u_0 = \eta/\sqrt{3}$). The associated velocities $w = 4\kappa u/\delta$ are, for $B/\eta = 1/3, 6$ and 2 cm/yr, for the long- and short-plate solutions, respectively.

Although $\nu = C/\mathcal{K}^2$ is small, it influences the steady state solutions, which are found numerically (see Figure 2a). While the range of solutions for u_0 do not change, they occur for smaller values of B . For $\nu \approx 0.1$, the range of allowable B is $0.1 \leq B/\eta \leq 0.19$, which corresponds to the viscosity ratio range $8 \leq \mu/\mu_0 \leq 16$. Thus, the continental pile exerts enough resistance that steady solutions only exist if the lower mantle viscosity is reduced.

Although the two equilibrium solutions for u_0 have significantly different lengths and velocities, the associated widths of the continental pile $r_0 = \mathcal{K}u_0^{-1/5}$ have little variation. The ratio of the continental widths for the shortest- and longest-plate states (given by $u_0 = (2 \pm 1)\eta/3$) is simply $3^{1/5} \approx 1.25$. Thus, the continental pile lengthens by 25% from one equilibrium state to the other.

3.2. Stability

The rollback instability is inferred from the stability of the equilibrium solutions (u_0, r_0) from section 3.1. Substituting infinitesimal perturbations to these solutions $(u, r) = (u_0, r_0) + \epsilon(u_1(t), r_1(t))$, where $\epsilon \ll 1$, into (9), we obtain to $\mathcal{O}(\epsilon^1)$:

$$\frac{du_1}{dt} = \left(1 - \frac{C}{\mathcal{K}^2} u_0^{2/5}\right) \frac{3u_0^2 - \eta^2}{3u_0(u_0 - \eta) + \eta^2} u_1 + \frac{2Cu_0^{8/5}}{\mathcal{K}^3} r_1 \quad (13a)$$

$$\frac{dr_1}{dt} = -\frac{\mathcal{K}}{u_0^{1/5}} u_1 - 5u_0 r_1 \quad (13b)$$

Using $(u_1, r_1) \sim e^{st}$ in (13), we infer a quadratic relation for the growth rate s and thus two growth rates for each of the two steady solutions u_0 . For the case of $\nu = C/\mathcal{K}^2 \ll 1$, only the evolution equation for u_1 is needed and

$$s = \frac{3u_0^2 - \eta^2}{3u_0(u_0 - \eta) + \eta^2} \quad (14)$$

In the case of $B = \eta/3$ and $u_0 = (2 \pm 1)\eta/3$, the growth rates are $s = \pm 2$; i.e., the equilibrium long-plate solution $u_0 = \eta$ is unstable while the short-plate solution $u_0 = \eta/3$ is stable. The maximum growth rate

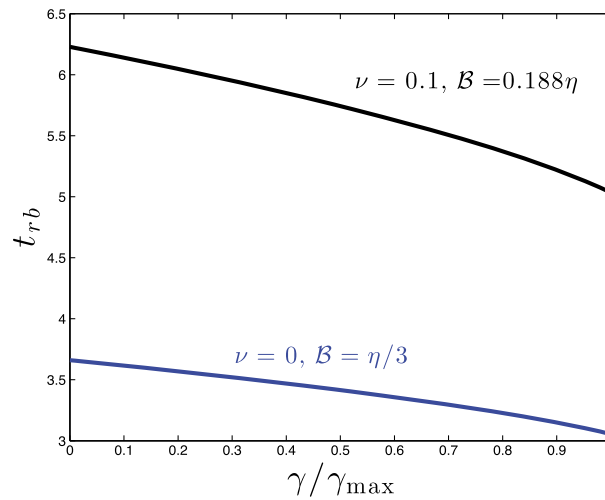


Figure 4. Total time for rollback t_{rb} from (16) between the two equilibrium states (i.e., the long, unstable plate and the short, stable plate) versus the rollback dissipation parameter γ and for cases with ($\nu > 0$ black line) and without ($\nu = 0$, blue line) continental drag; γ is normalized by the corresponding γ_{max} from Figure 3. The parameter B is chosen to allow the equilibrium states $u_0 \approx (2 \pm 1)\eta/3$. Since (16) is singular at the equilibrium states, the integration limits are evaluated at $(2 \pm 1)\eta/3 \cdot (1 \mp \epsilon)$, where for the cases shown $\epsilon = 10^{-2}$.

s_{max} for general B and $\nu = C/\mathcal{K}^2$ (Figure 2b) reveals that the long-plate state is always unstable, while the short-plate one is stable. Thus, the supercontinent slab configuration is unstable, and the slabs retreat to a stable state with shorter plates. The process of rolling back, and the associated in-fill of mass between the two retreating slabs, would then disperse the continent between the slabs.

3.3. Rollback Velocity

The nonlinear evolution equations (9) can be used to infer the rollback velocity du/dt as the trench retreats from the long- to short-plate states. For the simple case with $\nu = C/\mathcal{K}^2 \ll 1$ the governing equations are decoupled and du/dt is only a function of u . For the general case of $\nu > 0$, we assume that $dr/dt \approx 0$; i.e., since both terms on the right side of (9b) are very large, they are likely much bigger than their difference dr/dt . In this case, using $r \approx \mathcal{K}u^{-1/5}$ in (9a), we obtain a closed and integrable relation for the rollback velocity:

$$\frac{du}{dt} = \mathcal{F}(u) = \frac{u(\eta - u)}{4\gamma B} \left(-1 + \sqrt{1 + \frac{8\gamma B}{\eta - u} \left(1 - \nu u^{2/5} - \frac{3B\eta u}{u^3 + (\eta - u)^3} \right)} \right) \quad (15)$$

(Figure 3). (We also verify the assumption that $dr/dt \approx 0$ for cases with $\nu > 0$ by comparing (15) to full numerical solutions of (9); see Figure 3b.) The rollback velocity is negative as the system evolves from the long- to short-plate equilibria. (In principle, trench advance could occur if the initial plate is longer than in the unstable equilibrium state, but in that case there is no stable state to which it can evolve.) In all cases, the maximum absolute rollback velocity $|du/dt|$ is comparable to but generally less than the peak plate velocity u (which agrees with Schellart *et al.* [2007]) and occurs roughly at the midpoint between the two equilibrium lengths of u (recall that u represents both dimensionless plate speed and length). At these velocities, the rollback instability can disperse continental crust at a tectonically feasible rate.

3.4. Rollback Time

The integration of (15) between the long-plate and short-plate equilibrium states gives the net rollback time

$$t_{rb} = \int_{u_{0_l}}^{u_{0_s}} \frac{du}{\mathcal{F}(u)} \quad (16)$$

where the u_{0_j} are the long- ($j = l$) and short-plate ($j = s$) equilibrium solutions. The rollback time appears most sensitive to the continental drag factor $\nu = C/\mathcal{K}^2$ (Figure 4). Using $\mathcal{R}_c \approx 660$ and properties from Table 1, the dimensional rollback time is typically 200–400 Myrs, which is commensurate with the age of ocean basins and the period of the Wilson cycle.

4. Summary and Conclusion

Trench migration plays an important role in mantle flow patterns, back-arc deformation and volcanism, and arc/slab morphology in subduction systems [Lallemand *et al.*, 2008; Clark *et al.*, 2008; Long and Silver, 2009; Stegman *et al.*, 2010; Long *et al.*, 2012; Cramer and Tackley, 2014]; we suggest that it may also play a crucial role in the supercontinent cycle. In particular, our simple theory illustrates how a “supercontinent” configuration of subduction zones is naturally unstable to slab rollback and trench retreat and evolves to a stable state of dispersed slabs and continents. This mechanism provides an alternative to continental dispersal via

mantle thermal insulation and induced upwelling [e.g., Gurnis, 1988; Lenardic et al., 2011; Yoshida, 2013], which is problematic if the mantle Urey number is small [Korenaga, 2008; Jaupart et al., 2007]. In contrast, our proposed rollback instability is purely mechanical and independent of heating mode. Moreover, the slab rollback velocity implied by the model is comparable to typical tectonic plate velocities; hence the rollback time (to go from the unstable supercontinent state to the stable dispersed-continent state) is comparable to the age of ocean basins and the Wilson cycle period. The model is idealized in that it is 2-D, neglects possible effects of complex rheology and strength in the lithosphere (leading to self-weakening and/or strong continental lithosphere), and does not account for the agglomeration cycle, which we assume is inevitably driven by convergence over convective downwellings (although whether by “extroversion or “introversion” remains debated [e.g., Murphy et al., 2009]). Nevertheless, our simple model provides feasible predictions for supercontinent dispersal and a framework for further, more sophisticated investigations.

Acknowledgments

The paper benefitted from helpful comments by Taras Gerya and an anonymous reviewer. Support was provided by NSF-FESD award EAR-1135382: Open Earth Systems. Numerical solutions were obtained using standard Matlab routines, and the associated scripts can be requested from the corresponding author (DB).

The Editor thanks two anonymous reviewers for their assistance in evaluating this paper.

References

- Anderson, D. L. (1982), Hotspots, polar wander, mesozoic convection and the geoid, *Nature*, 297(5865), 391–393.
- Becker, T., C. Conrad, B. Buffett, and R. Müller (2009), Past and present seafloor age distributions and the temporal evolution of plate tectonic heat transport, *Earth Planet. Sci. Lett.*, 278, 233–242.
- Bercovici, D., and Y. Ricard (2012), Mechanisms for the generation of plate tectonics by two-phase grain-damage and pinning, *Phys. Earth Planet. Int.*, 202–203, 27–55, doi:10.1016/j.pepi.2012.05.003.
- Bercovici, D., and Y. Ricard (2014), Plate tectonics, damage and inheritance, *Nature*, 508, 513–516, doi:10.1038/nature13072.
- Chandrasekhar, S. (1961), *Hydrodynamic and Hydromagnetic Stability*, Oxford Univ. Press, New York.
- Clark, S. R., D. Stegman, and R. D. Müller (2008), Episodicity in back-arc tectonic regimes, *Phys. Earth Planet. Inter.*, 171(1–4), 265–279, doi:10.1016/j.pepi.2008.04.012.
- Cramer, F., and P. J. Tackley (2014), Spontaneous development of arcuate single-sided subduction in global 3-D mantle convection models with a free surface, *J. Geophys. Res. Solid Earth*, 119, 5921–5942, doi:10.1002/2014JB010939.
- Didden, N., and T. Maxworthy (1982), The viscous spreading of plane and axisymmetric gravity currents, *J. Fluid Mech.*, 121, 27–42, doi:10.1017/S00222112082001785.
- Funiciello, F., M. Moroni, C. Piromallo, C. Faccenna, A. Cenedese, and H. A. Bui (2006), Mapping mantle flow during retreating subduction: Laboratory models analyzed by feature tracking, *J. Geophys. Res.*, 111, B03402, doi:10.1029/2005JB003792.
- Gerya, T. V., and F. I. Meilick (2011), Geodynamic regimes of subduction under an active margin: Effects of rheological weakening by fluids and melts, *J. Metamorph. Geol.*, 29(1), 7–31, doi:10.1111/j.1525-1314.2010.00904.x.
- Gurnis, M. (1988), Large-scale mantle convection and the aggregation and dispersal of supercontinents, *Nature*, 332(6166), 695–699, doi:10.1038/332695a0.
- Gurnis, M., C. Hall, and L. Lavier (2004), Evolving force balance during incipient subduction, *Geochem. Geophys. Geosyst.*, 5, Q07001, doi:10.1029/2003GC000681.
- Heron, P. J., and J. P. Lowman (2011), The effects of supercontinent size and thermal insulation on the formation of mantle plumes, *Tectonophysics*, 510(1–2), 28–38, doi:10.1016/j.tecto.2011.07.002.
- Howard, L. N. (1966), Convection at high Rayleigh number, in *Proceedings of the Eleventh International Congress of Applied Mechanics*, edited by H. Gortler, pp. 1109–1115, Springer-Verlag, New York.
- Huppert, H. (1982), The propagation of two-dimensional and axisymmetric viscous gravity currents over a rigid horizontal surface, *J. Fluid Mech.*, 121, 43–58.
- Jaupart, C., S. Labrosse, and J.-C. Mareschal (2007), Temperatures, heat and energy in the mantle of the Earth, in *Treatise on Geophysics Volume 7: Mantle Dynamics*, edited by D. Bercovici and G. Schubert, pp. 253–303, Elsevier, New York.
- Kincaid, C., and R. W. Griffiths (2003), Laboratory models of the thermal evolution of the mantle during rollback subduction, *Nature*, 425(6953), 58–62.
- Korenaga, J. (2008), Urey ratio and the structure and evolution of Earth's mantle, *Rev. Geophys.*, 46, RG2007, doi:10.1029/2007RG000241.
- Lallemand, S., A. Heuret, C. Faccenna, and F. Funiciello (2008), Subduction dynamics as revealed by trench migration, *Tectonics*, 27, TC3014, doi:10.1029/2007TC002212.
- Lenardic, A., L. Moresi, A. M. Jellinek, C. J. O'Neill, C. M. Cooper, and C. T. Lee (2011), Continents, supercontinents, mantle thermal mixing, and mantle thermal isolation: Theory, numerical simulations, and laboratory experiments, *Geochem. Geophys. Geosyst.*, 12, Q10016, doi:10.1029/2011GC003663.
- Long, M. D., and P. G. Silver (2009), Mantle flow in subduction systems: The slab flow field and implications for mantle dynamics, *J. Geophys. Res.*, 114, B10312, doi:10.1029/2008JB006200.
- Long, M. D., C. B. Till, K. A. Druken, R. W. Carlson, L. S. Wagner, M. J. Fouch, D. E. James, T. L. Grove, N. Schmerr, and C. Kincaid (2012), Mantle dynamics beneath the Pacific Northwest and the generation of voluminous back-arc volcanism, *Geochem. Geophys. Geosyst.*, 13, Q0AN01, doi:10.1029/2012GC004189.
- Murphy, J. B., R. D. Nance, and P. A. Cawood (2009), Contrasting modes of supercontinent formation and the conundrum of Pangea, *Gondwana Res.*, 15(3–4), 408–420, doi:10.1016/j.gr.2008.09.005.
- Nikolaeva, K., T. V. Gerya, and F. O. Marques (2010), Subduction initiation at passive margins: Numerical modeling, *J. Geophys. Res.*, 115, B03406, doi:10.1029/2009JB006549.
- Piromallo, C., T. W. Becker, F. Funiciello, and C. Faccenna (2006), Three-dimensional instantaneous mantle flow induced by subduction, *Geophys. Res. Lett.*, 33, L08304, doi:10.1029/2005GL025390.
- Rolf, T., and P. J. Tackley (2011), Focussing of stress by continents in 3D spherical mantle convection with self-consistent plate tectonics, *Geophys. Res. Lett.*, 38, L18301, doi:10.1029/2011GL048677.
- Rolf, T., N. Coltice, and P. J. Tackley (2012), Linking continental drift, plate tectonics and the thermal state of the Earth's mantle, *Earth Planet. Sci. Lett.*, 351, 134–146, doi:10.1016/j.epsl.2012.07.011.
- Rolf, T., N. Coltice, and P. J. Tackley (2014), Statistical cyclicity of the supercontinent cycle, *Geophys. Res. Lett.*, 41(7), 2351–2358, doi:10.1002/2014GL059595.

- Schellart, W., D. Stegman, and J. Freeman (2008), Global trench migration velocities and slab migration induced upper mantle volume fluxes: Constraints to find an Earth reference frame based on minimizing viscous dissipation, *Earth Sci. Rev.*, *88*(1–2), 118–144, doi:10.1016/j.earscirev.2008.01.005.
- Schellart, W. P., J. Freeman, D. R. Stegman, L. Moresi, and D. May (2007), Evolution and diversity of subduction zones controlled by slab width, *Nature*, *446*(7133), 308–311.
- Solomatov, V. (1995), Scaling of temperature dependent and stress dependent viscosity convection, *Phys. Fluids*, *7*, 266–274.
- Stegman, D., R. Farrington, F. Capitanio, and W. Schellart (2010), A regime diagram for subduction styles from 3-D numerical models of free subduction, *Tectonophysics*, *483*(1–2), 29–45, doi:10.1016/j.tecto.2009.08.041.
- Stegman, D. R., J. Freeman, W. P. Schellart, L. Moresi, and D. May (2006), Influence of trench width on subduction hinge retreat rates in 3-D models of slab rollback, *Geochem. Geophys. Geosyst.*, *7*, Q03012, doi:10.1029/2005GC001056.
- Wilson, J. (1966), Did the Atlantic close and then re-open?, *Nature*, *211*, 676–681.
- Yoshida, M. (2010), Preliminary three-dimensional model of mantle convection with deformable, mobile continental lithosphere, *Earth Planet. Sci. Lett.*, *295*(1–2), 205–218, doi:10.1016/j.epsl.2010.04.001.
- Yoshida, M. (2012), Dynamic role of the rheological contrast between cratonic and oceanic lithospheres in the longevity of cratonic lithosphere: A three-dimensional numerical study, *Tectonophysics*, *532–535*, 156–166, doi:10.1016/j.tecto.2012.01.029.
- Yoshida, M. (2013), Mantle temperature under drifting deformable continents during the supercontinent cycle, *Geophys. Res. Lett.*, *40*(4), 681–686, doi:10.1002/GRL.50151.
- Yoshida, M., and M. Santosh (2011), Supercontinents, mantle dynamics and plate tectonics: A perspective based on conceptual vs. numerical models, *Earth Sci. Rev.*, *105*(1–2), 1–24, doi:10.1016/j.earscirev.2010.12.002.